Chapter 4

Solution Combustion Synthesis and Structural Studies of Rocksalt High Entropy Oxide (Mg,Co,Ni,Cu,Zn)O

4.1 Introduction

The concept of high entropy alloys has recently extended to oxides when equimolar (Mg,Co,Ni,Cu,Zn)O was synthesised using through ball milling MgO, CoO, NiO, CuO, and ZnO in the solid state [22]. The ball milled oxide mixture was subsequently annealed to a temperature >875 ℃ to obtain the high entropy rocksalt phase. Since then, HEOs have been synthesised using various techniques, including solid-state synthesis [2,126], nebulized spray pyrolysis (NSP) [92,114], flame spray synthesis (FSP) [57,92], hydrothermal [120,195] and co-precipitation [57,92,114]. However, in all the cases, a single-phase could only be obtained after annealing at higher temperatures (usually >875 ℃).

Solution Combustion Synthesis (SCS) is a versatile and energy-efficient method for producing advanced materials, including ceramics, catalysts, and functional oxides[119,187]. The process begins with the preparation of a homogeneous solution of precursor compounds, typically consisting of metal salts (as oxidizers) and an organic fuel (as a reductant), dissolved in a suitable solvent. Initial heating causes the solvent to evaporate, leading to the drying of the precursor mixture. Subsequently, the precursor compounds decompose thermally, releasing volatile

species such as water vapor, carbon dioxide, and ammonia [196]. This decomposition lowers the energy barrier for the next stages of the reaction. In this stage, once decomposition begins, the system reaches a critical temperature where the fuel exothermically reacts with the oxidizer releasing heat. Due to the exothermic nature, the reaction propagates rapidly through the material as self-sustaining combustion wave [197]. The localized heat generated during this process can exceed 900°C, which would be sufficient to facilitate the nucleation and crystallization of the rocksalt HEO. To stabilize the rocksalt solid solution phase ($\Delta G < 0$), conventional methods rely on annealing above 850°C, allowing the entropy term ($T\Delta S$ in $\Delta G = \Delta H - T\Delta S$) to overcome the positive enthalpy of mixing (ΔH) [45,97,198]. Moreover, techniques such as FSP and NSP demand complex setups and are energy-intensive. Thus, developing a cost-effective and easily controlled synthesis method is essential to make these materials more accessible for research and innovation.

In this chapter we investigated effect of fuel utilized during SCS on the phase evolution in five component (Mg,Co,Ni,Cu,Zn)O rocksalt HEO. The as-synthesized powders using citrate gel SCS had ~85% high entropy rocksalt phase along with tenorite (CuO) and wurtzite (ZnO) phases. Upon annealing at elevated temperature, the unary oxide phases gradually dissolved, culminating in the formation of a phase-pure high-entropy rocksalt solid solution at temperatures exceeding 850°C. On the other hand, when glycine ($C_2H_5NO_2$) is utilized as a combusting fuel, SCS resulted in a phase pure five-component HEOs

(Mg,Co,Ni,Cu,Zn)O at the combustion temperature of 185 °C without the need of post-annealing.

4.2 Experimental

4.2.1 Materials preparation

For solution combustion synthesis of HEO, two different fuels, citric acid and glycine, were utilized. In the case of citric acid, fuel to oxidizer ratio Φ = 1 and pH ~10 was maintained, whereas in the case of glycine ($C_2H_5NO_2$), a relatively lean mixture (fuel to oxidizer ratio Φ = 0.8) was maintained to control the combustion rate and the synthesis was carried out at varying pH of solutions 1, 5, 7, and 10.

4.2.2 Characterization

XRD patterns were recorded in 2θ range from 20° to 80° with a step size of 0.02 and a scan rate of 2°/min. Differential scanning calorimetry (DSC) (Shimadzu (Asia Pacific) Pte Ltd. Model-DSC-60, USA, set up calibrated with 10 mg of alumina) was carried out by heating the samples in air (100 ml/min) at 10 °C/min from 25 to 420 °C. The differential thermal analysis (DTA) and thermogravimetric analysis (TGA) (EXSTAR TG/DTA 6300) was carried out in air (flow rate 200 ml/min) at 5 °C/min from 25 °C to 1000 °C. The phase evolution and lattice parameters were analyzed by the Rietveld Method using the GSAS-II software suit. To identify the functional groups, present during different stages of synthesis, Fourier transform infrared spectroscopy (FTIR (Model-Tensor II, Bruker, USA) was carried out.

4.3 Results and Discussion

4.3.1 Combustion synthesis with citric Acid

Citric acid ($C_6H_8O_7$), when used as a fuel in solution combustion synthesis (SCS), typically undergoes an exothermic reaction releasing heat. If the heat energy released is sufficient, the adiabatic temperature due to fuel oxidation can increase at a high rate to the critical temperature, forming single phase rocksalt structure. On the other hand, if exothermic energy released is not sufficient then a multiple phase mixture can form. During combustion using citric acid following reaction takes place:

$$0.2Mg(NO_3)_2 + 0.2Co(NO_3)_2 + 0.2Ni(NO_3)_2 + 0.2Cu(NO_3)_2 + 0.2Zn(NO_3)_2 + (5/9)C_6H_6O_7 \rightarrow (Mg,Co,Ni,Cu,Zn)\ O + (20/9 + 6)H_2O + N_2 + (10/3)CO_2 \quad (1)$$

The heat of combustion reaction was calculated using the relation:

$$\Delta H_{Combustion} = (\Delta H_f)_{Product} - (\Delta H_f)_{Reactant} \quad (2)$$

The adiabatic combustion temperature (T_{ad}) was estimated using eq. (3).

$$\Delta H_{Combustion} = \int_{298}^{T} \sum (nCp)_{Products} \quad (3)$$

The enthalpy of formation for the products ($(\Delta H_f)_{Product,}$) and reactants ($(\Delta H_f)_{Reactant}$) was estimated to be -3248.05 kJ/mol·K and -2976.93 kJ/mol·K, respectively. $\Delta H_{Combustion}$ estimated for the reaction was 271.2 kJ/mol and the adiabatic combustion temperature (T_{ad}) was approx. 907 °C. The Differential Scanning Calorimetry (DSC) thermogram of the dried gel, shown in **Figure 4.1 (a)**, reveals

key thermal events. An endothermic peak at ~100°C corresponds to water desorption. A prominent exothermic peak around ~230°C, accompanied by smaller shoulder-like exothermic peaks, is associated with the combustion and oxidation of the citric complex and residual citrate [199]. Additionally, a minor endothermic peak near 350 °C is attributed to the decomposition of residual nitrate complexes or remaining citric acid. The XRD pattern of the as-synthesized powder (obtained after auto-combustion at 230 °C) is presented in **Figure 4.1 (b)**. The presence of distinct, sharp peaks and the absence of diffuse peaks confirm that the combustion process produced a crystalline material [25]. Although the estimated adiabatic temperature was comparable to 900°C during combustion however phase pure rocksalt was not achieved. Which ascribe to slow rate of combustion in citrate gel combustion results in heat loss. Most of the peaks correspond to three primary phases: rocksalt structure, tenorite (CuO), and wurtzite (ZnO). This observation suggests that the heat generated during citrate combustion was insufficient to elevate the temperature and consequently, the TΔS term to offset the positive enthalpy of dissolution required for the formation of a single-phase solid solution [45]. The oxides NiO, MgO, and CoO, which naturally adopt a rocksalt structure, readily dissolve to form an extensive solid solution [49,97]. However, ZnO and CuO crystallize as wurtzite and tenorite, respectively, and must undergo phase transformations to the rocksalt structure to dissolve. These transformations involve a positive enthalpy change, further complicating their incorporation. To identify the temperature at which the TΔS term becomes sufficient to overcome this positive enthalpy, the powders were annealed at various temperatures and rapidly quenched

[151]. The phase evolution was subsequently monitored through XRD analysis of the annealed powders, as shown in **Figure 4.1(c)**.

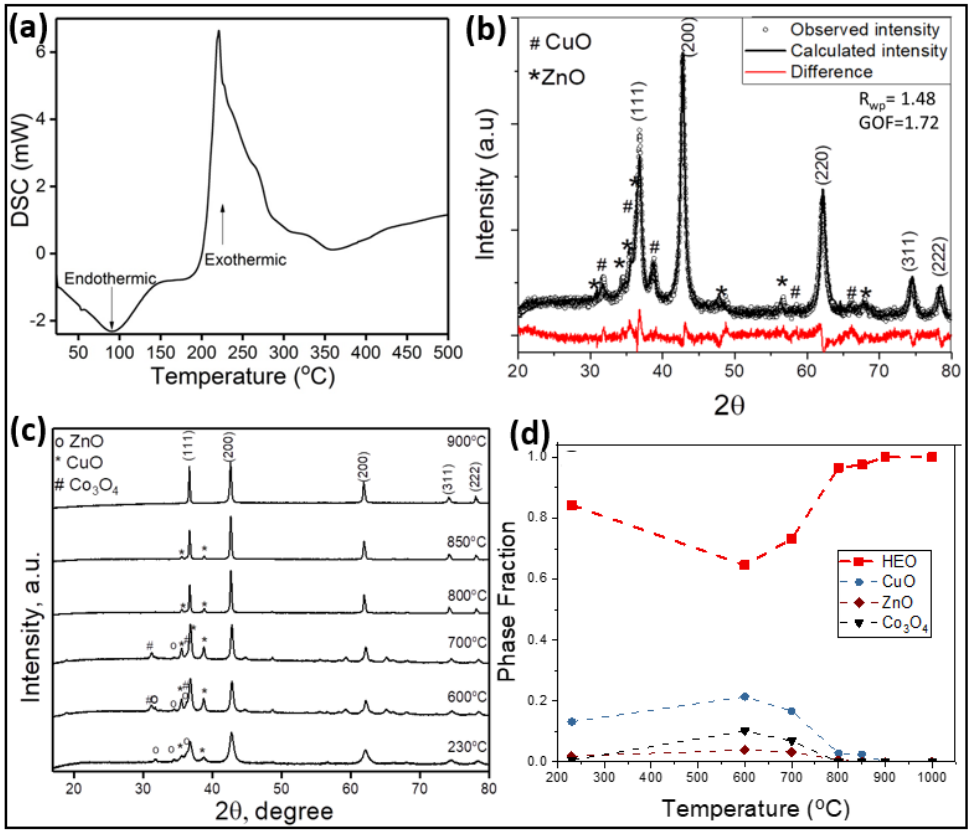

Figure 4.1(a) DSC thermogram of the dried gel of metal nitrate precursor mixed with citric acid in SCS, indicating exothermic auto-combustion reaction at 250°C. (b) XRD pattern of the powder after combustion at 230 ºC indicating rocksalt as major phase along with tenorite (CuO) and wurtzite (ZnO) as minor phase (c) XRD patterns of the powder after combustion and calcined at different temperatures varying from 600 to 900 ºC (d) depicts Quantitative phase evolution in five component HEO at different temperature.

Phase quantification was performed using the Rietveld refinement method in GSAS II, with the fitted XRD patterns. The refinement yielded excellent fitting parameters (Rwp < 3% and χ^2 between 1.5-3.0) across all samples. The phase fractions as a function of annealing temperature are shown in **Figure 4.1 (d)**. The as-synthesized powder comprised of ~84% rocksalt ($Fm\bar{3}m$) phase, ~13% tenorite (CuO), and ~2% wurtzite (ZnO), with trace amounts of Co_3O_4 (<1%). Upon annealing at 600 °C, the phase composition changes to include ~65% rocksalt, ~21% tenorite, ~10% Co_3O_4 (spinel), and ~4% wurtzite. Notably, the Co_3O_4 spinel phase emerged prominently alongside ZnO and CuO. Further annealing at 700 °C results in a decline in the fractions of tenorite, spinel, and wurtzite, while the rocksalt phase fraction increases to ~73%. At 800 °C, the Co_3O_4 spinel phase disappears entirely, indicating its dissolution into the high entropy rocksalt phase[190]. Meanwhile, the fractions of tenorite and wurtzite decrease significantly to ~3% and <1%, respectively, this phase evolution highlights that, at 800 °C all phases except tenorite (CuO) dissolves into the rocksalt phase. The persistence of CuO can be attributed to its higher enthalpy of transformation (~25 kJ/mol) compared to ZnO (~22 kJ/mol) [22]. Additionally, ZnO adopts a rocksalt structure under high-pressure conditions, facilitating its dissolution into the rocksalt phase at ~700°C. In contrast, the greater enthalpy of transformation for CuO necessitates higher temperatures to achieve complete dissolution into the mixed oxide. To ensure the complete dissolution of the tenorite phase into the solid solution, the powders were annealed at higher temperatures to increase the $T\Delta S$ term, thereby compensating for the positive enthalpy of transformation. When heated to 850°C, the sample primarily exhibits a single-phase rocksalt structure with only minor traces of tenorite remaining. Further

annealing at 900°C results in the complete disappearance of any unary oxide phases, with the XRD pattern exclusively indexing to the rocksalt phase. The dissolution of all five metallic ions with varying atomic radii significantly impacts the cell parameter of the rocksalt structure. Co^{2+} (0.72 Å) and Ni^{2+} (0.70 Å) have slightly smaller ionic radii in octahedral co-ordination when compared to Mg^{2+} (0.72 Å), while Zn^{2+} (0.74 Å) and Cu^{2+} (0.73 Å). This changes the lattice parameter as a function of temperature. As CuO, ZnO, and Co_3O_4 dissolve between 600-800°C and given the positive ΔH of mixing for CuO and ZnO an increase in the lattice parameter is expected during this range. Indeed, the cell parameter increased from 4.214 ± 0.002 Å to 4.235 ± 0.002 Å during the dissolution process, stabilizing thereafter with no significant change upon further annealing at higher temperatures **(Figure 4.2)**.

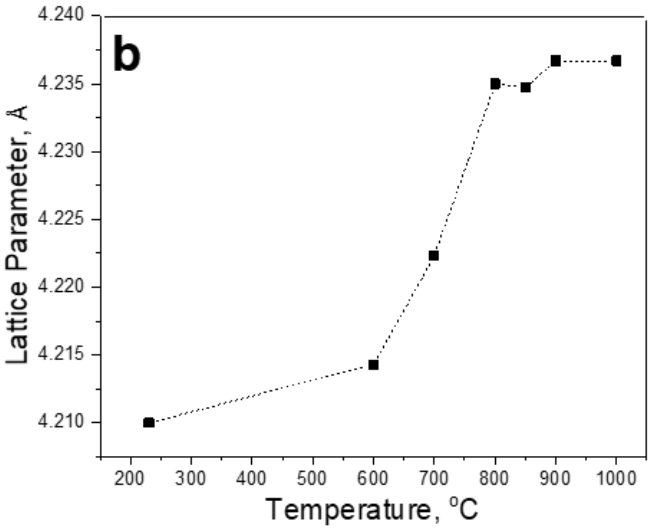

Figure 4.2 Variation in lattice parameter with annealing temperature.

The positive enthalpy of dissolution was corroborated by the differential Thermal Analysis (DTA) thermogram shown in **Figure 4.3a**. The DTA thermogram of the

powder, pre-calcined at 600°C, display an endothermic peak centered around 725°C, spanning the temperature range of 600-800°C. This temperature range aligns with the dissolution of the majority of unary oxides. Additionally, thermogravimetric Analysis (TGA), shown in **Figure 4.3a** (below), revealed no significant mass loss between 700-900 °C, confirming that the observed endothermic peak in the DTA thermogram (**Figure 4.3a** (above)) corresponds to the dissolution of the remaining oxides, rather than any thermal decomposition or volatilization. Thermogravimetric (TG) analysis shows no significant mass loss in the 700-900°C range, confirming that the endothermic peak observed in the DTA thermogram is due to the dissolution of the residual oxides rather than thermal decomposition or material loss. To understand the chelation and complex formation by citric acid, FTIR spectra were recorded for the dried gel, combusted, and calcined powders, as shown in Figure 4.2(b). In the dried gel, absorption bands at 1612 cm^{-1} and 1380 cm^{-2} are attributed to the asymmetric and symmetric vibrations of the carboxyl group in the citrate complex, while the band at 1577 cm^{-2} corresponded to -C=O bonds[199]. The absorption band at 3190 cm^{-1} is associated with -OH groups, and the broad band at 3388 cm^{-2} is attributed to H_2O. Additional weaker bands at 1216, 1140, and 1070 cm^{-2} are assigned to N-O bonds.

These spectral features are consistent with those reported by Niu et al. [118]. Bands at shorter wavenumbers are linked to metal-oxygen bonding. After auto-combustion at 230°C, most organic absorption bands disappear, leaving two prominent bands at 1415 cm^{-1} and 1486 cm^{-1}, attributed to residual C-O bonds that does not completely escape[134]. Upon calcination at 600 °C, only two absorptions

bands remain at ~675 cm^{-1} and ~500 cm^{-1}, both Corresponding to metal-oxygen bonding, indicating the complete decomposition of organic residues and the formation of the oxide framework. Further, elemental map obtained from SEM-EDS of (Mg,Co,Ni,Cu,Zn)O synthesized by citrate gel method showing the uniform distribution of elements as shown in **Figure 4.4**.

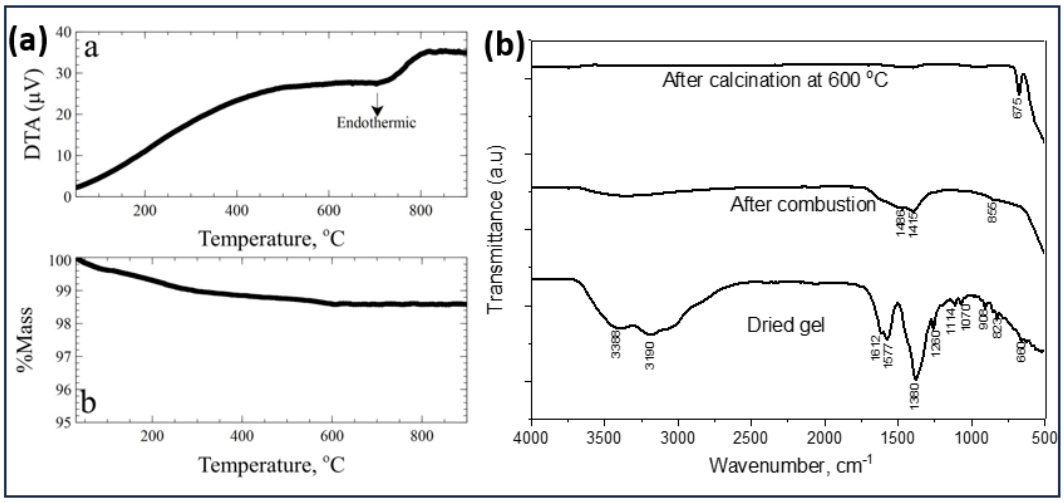

Figure 4.3 (a) TG-DTA plot of the powder calcined at 600 ºC. (b) FTIR of the dried gel, powder after combustion, and calcined powder.

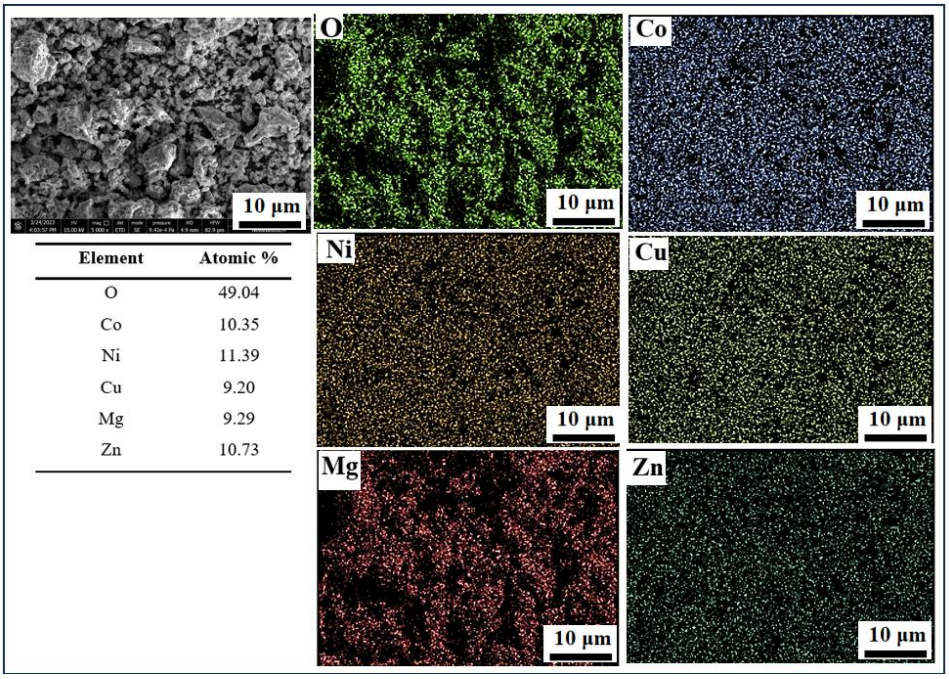

Figure 4.4 Elemental map obtained from SEM-EDS of (Mg,Co,Ni,Cu,Zn)O synthesized by citrate gel method showing the uniform distribution of elements.

4.3.2 Combustion synthesis with glycine

One of the aims of the work was to generate sufficient combustion temperatures (>850°C) to overcome the ΔH barrier, eliminating the need for a post-annealing process. Glycine, with a high rate of combustion compared to citric acid, could facilitate a rapid and a more vigorous combustion reaction [189,192,200]. Therefore, glycine fuel was utilized for the synthesis of high entropy oxide phase. During auto-combustion, the following chemical reaction takes place to yield HEO nanocrystalline powder.

$$0.2Co(NO_3)_2 + 0.2Cu(NO_3)_2 + 0.2Mg(NO_3)_2 + 0.2Ni(NO_3)_2 + 0.2Zn(NO_3)_2 + 5/2(\Phi\text{-}1)O_2 + (10\Phi/9)C_2H_5NO_2 \rightarrow (Mg,Co,Cu,Ni,Zn)O + (25\Phi/9)H_2O + (1+5\Phi/9)N_2 + (20\Phi/9)CO_2 \quad (4)$$

where, Φ (=0.8) indicates fuel to oxidizer ratio and in our experiments. Moreover, to control the rate of combustion the pH of the solution was adjusted using ammonia solution (28%) [199]. The solution of metal nitrate and glycine was continuously stirred for 24 h to obtain a blue gel which was subsequently dried at 80°C. Subsequently, the temperature raised slowly until auto combustion occurred, which happened at 185°C. The synthesis was carried out at varying pH of solutions 1, 5, 7, and 10.

The enthalpy of formation for the products ($(\Delta H_f)_{Product,}$) and reactants ($(\Delta H_f)_{Reactant}$) was calculated to be -3005.81 kJ/mol·K and -2757.25 kJ/mol·K, respectively, resulting in an estimated $\Delta H_{Combustion}$ of approximately -248.56 kJ/mol·K. The adiabatic temperature generated during combustion is estimated to be 867°C. The exothermic nature in glycine combustion is more intense and faster compared to citric acid, as glycine contains amino group ($-NH_2$) which reduces activation energy of reaction. XRD pattern of synthesized (Mg,Co,Ni,Cu,Zn)O nanocrystalline powders obtained after auto-combustion at varying pH values is shown in **Figure 4.5**, featuring sharp peaks on a smooth background, confirming the formation of well-crystallized powders. The prominent peaks could be indexed to a single-phase rocksalt structure ($Fm\bar{3}m$) with lattice parameter 4.235 ± 0.002 Å, verifying the successful synthesis of five-component rocksalt HEO. From the XRD it is clear that sample synthesized at pH 5 yields a phase-pure HEO (>99%) with no secondary phases, However, minor peaks corresponding to the tenorite (CuO) and wurtzite (ZnO) phases are detected in samples synthesized at pH 1, 7, and 10. This is due to the fact that the solutions combusted at pH 1, 7, and 10 could not completely remove

the organic ligands, which results in incomplete combustion reaction, leaving behind residual fuel and nitrate, as verified by the FTIR analysis shown in **Figure 4.6**. The absorption peaks corresponding to NO_3^- ions, O-H, C-H, and C=O bonds are notably weak in the sample synthesized at pH 5. The disappearance of these characteristic bands indicates that the NO_3^- ions from the metal nitrate and the functional groups from glycine are completely consumed during the combustion reaction at 185°C. This highly exothermic reaction generates sufficient heat to drive the formation of a single-phase HEO, eliminating the need for post-calcination. While XRD confirmed the formation of an entropy-stabilized single-phase rocksalt structure, the spatial uniformity of chemical species is equally critical for a multi-component high-entropy phase. To assess this, elemental distribution was analyzed using EDS coupled with SEM. As shown in **Figure 4.7**, the elemental maps for Mg, Co, Cu, Ni, and Zn reveal a uniform intensity across the examined area, confirming the homogeneous distribution of metals [190]. Additionally, the estimated atomic composition closely matches the equiatomic ratio. It is noteworthy that the calculated adiabatic temperature of the citrate combustion reaction was greater (907 °C) when compared to the glycine combustion (867 °C).

However, the combustion reaction of citric acid is slow and the heat release happens over a longer time. As a result, the condition is no longer adiabatic and the peak temperature calculated is not reached.

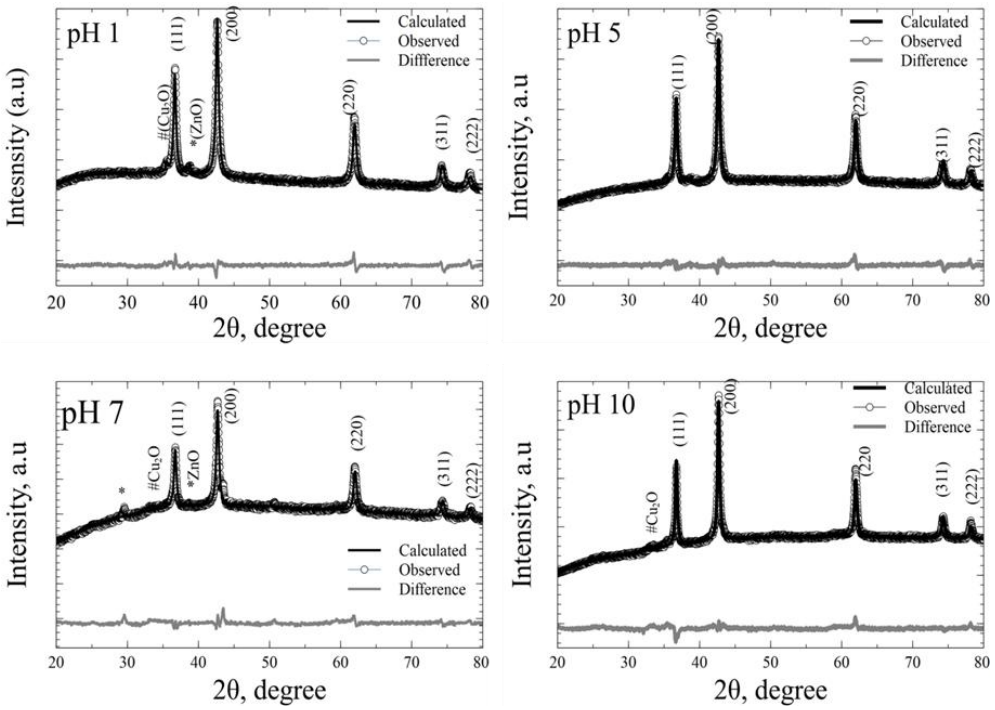

Figure 4.5 XRD pattern of the powders obtained after combustion at 185°C at varying pH.

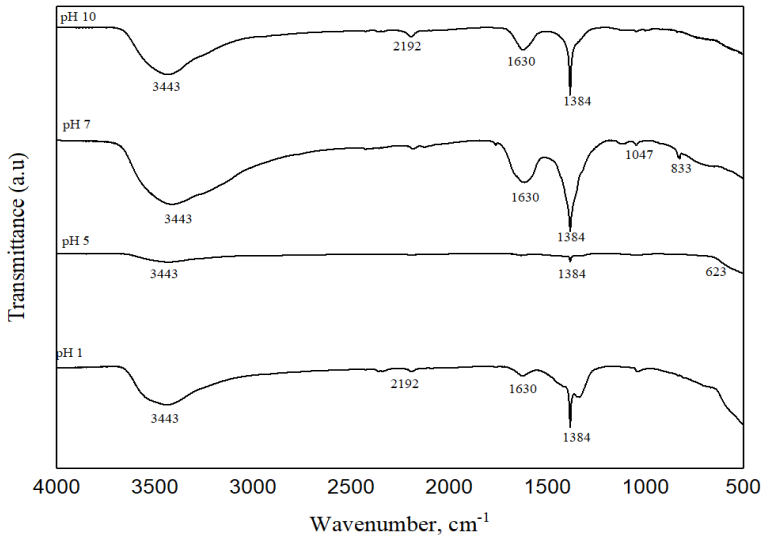

Figure 4.6 FTIR of powder synthesized at different pH values.

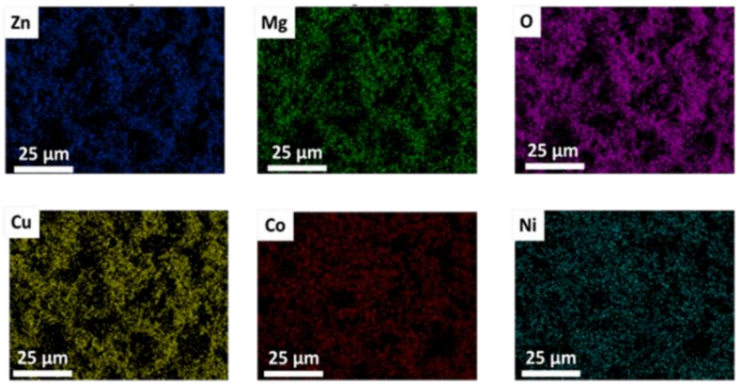

Element	Atomic%
O	49.73
Mg	8.29
Co	10.80
Ni	10.14
Cu	8.33
Zn	12.71

Figure 4.7 Elemental map obtained from SEM-EDS of (Mg,Co,Ni,Cu,Zn)O HEO powder synthesized from showing the uniform distribution of elements.

On the other hand, in the case of glycine, the exothermic reaction rate is fast, and the condition is closer to adiabatic, thereby increasing the TΔS term enough to overcome the ΔH of formation and stabilize the rocksalt phase.

4.4 Conclusions

To stabilize the rocksalt solid solution phase ($\Delta G < 0$), annealing above 850 °C is needed, allowing the entropy term ($T\Delta S$ in $\Delta G = \Delta H - T\Delta S$) to overcome the positive enthalpy of mixing (ΔH). The use of glycine as a fuel proved to be a more efficient synthesis route for single phase five component (Mg,Co,Ni,Cu,Zn)O HEO compared to citric acid. While the citric acid-based process generates comparable combustion temperature but reaction rate is slow compare to glycine and thus required a post-annealing step to achieve phase purity, The exothermic nature in glycine combustion is more intense and faster compared to citric acid, and thus raised the temperature high enough to form a single-phase HEO in a single step (during combustion), eliminating the need for additional thermal treatment. This

highlights the effectiveness of glycine in simplifying the synthesis process and reducing energy consumption.